Phoretic Interactions Generically Induce Dynamic Clusters
and Wave Patterns in Active Colloids

Benno Liebchen,[1,*] Davide Marenduzzo,[1] and Michael E. Cates[2]

[1]*SUPA, School of Physics and Astronomy, University of Edinburgh, Edinburgh EH9 3FD, United Kingdom*
[2]*DAMTP, Centre for Mathematical Sciences, University of Cambridge, Cambridge CB3 0WA, United Kingdom*

We introduce a representative minimal model for phoretically interacting active colloids. Combining kinetic theory, linear stability analyses, and a general relation between self-propulsion and phoretic interactions in autodiffusiophoretic and autothermophoretic Janus colloids collapses the parameter space from six to two dimensionless parameters: area fraction and Péclet number. This collapse arises when the lifetime of the self-generated phoretic fields is not too short, and leads to a universal phase diagram showing that phoretic interactions *generically* induce pattern formation in typical Janus colloids, even at very low density. The resulting patterns include waves and dynamic aggregates closely resembling the living clusters found in experiments on dilute suspension of Janus colloids.

Chemical signaling between cells is at the heart of many of the remarkable self-organization and pattern formation processes observed in the biological world. Microorganisms such as *Dictyostelium*, which excrete chemicals to which they respond themselves, provide an illustrative example of signaling-driven pattern formation. If they swim towards the signaling molecule (chemoattraction), any local accumulation of microorganisms causes an enhanced signal production, in turn recruiting further cells. This creates a positive feedback loop destabilizing the uniform phase (the Keller-Segel instability [1,2]) and leading to the formation of clusters which coarsen indefinitely. We recently found that a chemorepulsive response, where microorganisms swim away from the chemical they produce, provides an equally viable, if less intuitive, route to structure formation, resulting in clusters of self-limiting size, moving states and traveling waves [3].

A fascinating analog to biological signaling is provided by the collective behavior of synthetic autophoretic microswimmers. Such swimmers, often fabricated as Janus colloids, catalyze a chemical reaction on part of their surface and move in the resulting self-produced gradient by diffusiophoresis, or a similar mechanism. The resulting gradients then also act on other active particles, inducing chemically mediated (cross-phoretic) many-body interactions. By now, there are several models establishing the analogy between biological and synthetic signaling also formally [3–7].

One notable advantage of synthetic signaling swimmers over their biological counterparts is their conceptual simplicity and controllable design which should render parameter tuning simpler, offering new perspectives for active self-assembly (Fig. 1). Another advantage is that signaling in synthetic swimmers is not restricted to chemical interactions: thermophoretic Janus colloids [12], for

example, act as local heat sources and interact via self-produced temperature gradients. Despite this, as we shall see, they can be described by the same equations and allow access to different pattern forming regimes, not accessible for chemical signalers.

While it is widely believed that phoretic interactions between microswimmers can qualitatively lead to interesting collective behavior [3,4,13], little is known about the strength and relevance of these interactions in practical examples of autophoretic colloidal suspensions. Most notably, there are now several theoretically plausible mechanisms, based on phoretic concepts, driving the formation of the celebrated, yet mysterious, dynamic "living" clusters observed in low density suspensions of active colloids [14–17]. However, the lack of knowledge of the magnitude or even sign (attractive or repulsive) of the colloidal "chemotactic" (or thermotactic) coefficient makes it difficult to understand whether or not cross-phoretic interactions really induce the underlying instability.

To clarify this situation, the present work addresses the question of whether or not chemotactic instabilities are really there for generic autophoretic colloids. To address this, we introduce a representative minimal model for such colloids, the "phoretic Brownian particle" (PBP) model. The PBP model captures the impact of phoretic interactions on the orientations of other colloids, disregards additional but negligible cross-phoretic drift effects [4,6], and only requires one effective field rather than separate fuel and product fields.

Combining kinetic theory and linear stability analysis, we formulate generic instability criteria for Janus colloids whose phoretic interactions are either attractive (Keller-Segel instability [1,2]) or repulsive (Janus and delay-induced instabilities [3]). These criteria involve the microscopic parameters of the underlying Langevin
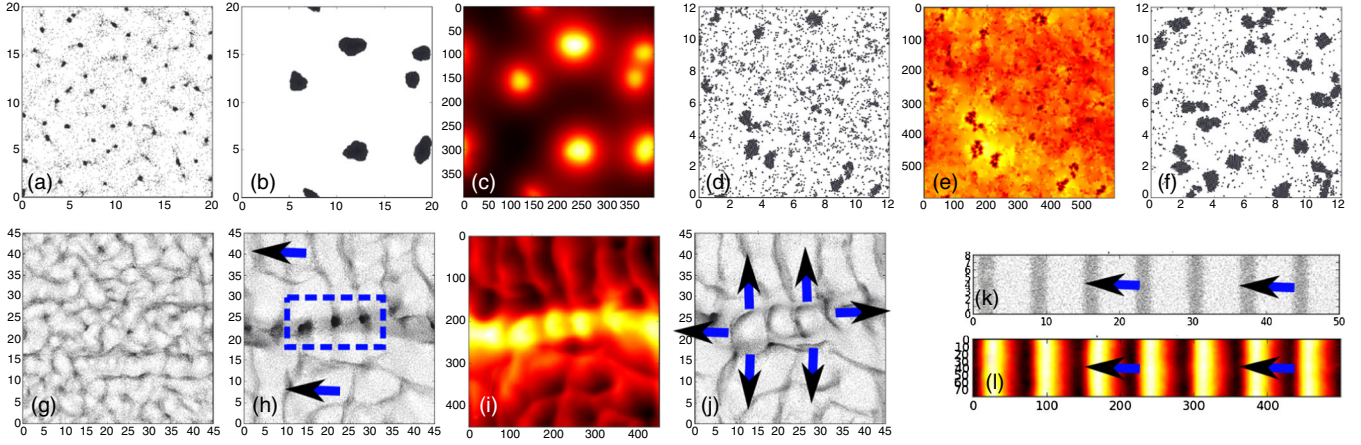
FIG. 1. Generic patterns in phoretic Janus colloids: snapshots from particle-based simulations (movies and parameters in the Supplemental Material [8]). (a–c, movie 1) Attractive phoretic interactions induce clusters at early times (s) which merge (b), accompanied by a colocated phoretic field (c). (d–f, movie 5) Dynamic clusters induced by repulsive phoretic interactions (d) surrounded by shells of large phoretic fields (e) which do not coarsen beyond a characteristic size (f). (g–l, movies 2–4) Colloidal waves (g) pursued by self-produced phoretic waves caging the colloids in dense clusters (h); these clusters act as enhanced phoretic producers leading to phoretic clusters (i) which drive colloids away, and induce escape waves (j). At late times, these wave patterns may settle into regular moving bands of colloids closely followed by phoretic waves (k,l).

equations, and are robust against short-range repulsions, as our large-scale particle-based simulations confirm.

As a key result, we unveil a general relation between self-propulsion and phoretic interactions in self-diffusiophoretic and self-thermophoretic Janus swimmers. This collapses the parameter space from six dimensions (after nondimensionalization) to two dimensions, and shows that *both* attractive and repulsive phoretic interactions *generically* induce structure formation in Janus colloids. Both are, therefore, generically important for the collective behavior of Janus colloids. In contrast to motility-induced phase separation in active Brownian particles (ABPs) [18] the phoretic patterns we discuss can occur at very low density providing an appealing mechanism to explain the onset of living clusters.

We consider N pointlike colloids confined to 2D (quasi-2D), moving with constant speed v due to self-propulsion along directions $\mathbf{p}_i = (\cos\theta_i, \sin\theta_i); i = 1, \ldots, N$. These swimming directions change due to rotational Brownian noise and coupling to a phoretic field c which is generated by all other colloids. This phoretic field is the one relevant for self-propulsion—a chemical or temperature field for diffusiophoretic or thermophoretic swimmers, respectively. (It may involve a combination of fuel and reaction products.) We define the PBP model by the equations of motion:

$$\dot{\mathbf{r}}_i(t) = v\mathbf{p}_i, \tag{1}$$

$$\dot{\theta}_i(t) = \beta\mathbf{p}_i \times \boldsymbol{\nabla}c + \sqrt{2D_r}\eta_i(t). \tag{2}$$

Here, D_r is the rotational diffusion constant and η represents unit-variance Gaussian white noise with zero mean; $\mathbf{a} \times \mathbf{b} \equiv a_1b_2 - a_2b_1$. The phoretic field c is produced at

rate k_0 by each colloid, and β quantifies the coupling to this phoretic field. When $\beta > 0$, particles turn towards the phoretic gradient produced by other colloids, modeling chemoattraction in diffusiophoretic colloids, whereas when $\beta < 0$ they swim down the gradient (chemorepulsion).

The phoretic field c evolves as

$$\dot{c}(\mathbf{r},t) = D_c\boldsymbol{\nabla}^2 c - k_d c + \sum_{i=1}^{N} \oint d\mathbf{x}_i \delta(\mathbf{r} - \mathbf{r}_i(t) - R_0\mathbf{x}_i)\sigma(\mathbf{x}_i). \tag{3}$$

While our colloids can be considered as mechanically pointlike (robustness of our results against short-range repulsions is shown below), finite particle sizes are crucial when describing phoretic interactions. Accordingly, the integral in (3) is over the 3D surface of the Janus colloids with radius R_0; the production rate density obeys $\sigma(\mathbf{x}_i) = k_0/(2\pi R_0^2)$ on the catalytic (coated) hemisphere and is zero elsewhere. Note that our results do not depend on a strictly hemispherical Janus design but are largely independent of the coating area and shape [8]. We also introduced the diffusion constant of the phoretic field D_c and allow for a decay of c with rate k_d representing chemical decay or heat losses to (bottom) container walls (for sedimented colloids) avoiding a divergence of c. This decay effectively gives screening effects, which we expect to be small when chemical decay is slow. To reduce the parameter space, we choose time and space units as $t_u = 1/D_r$ and $x_u = R_0$, leaving us with five dimensionless numbers alongside the particle density ρ_0: (i) the Péclet number $\mathrm{Pe} = v_0/(R_0 D_r)$, measuring the ballistic run length of a colloid in units of its radius; (ii) $B = \beta/(D_r R_0^4)$ comparing the phoretically
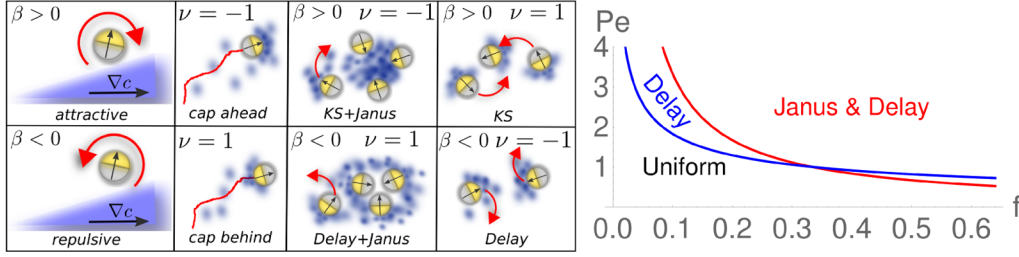
FIG. 2.   First set of four panels (from left): classification of autophoretic Janus colloids by their response to phoretic gradients (attractive and repulsive) and their swimming direction (cap ahead and behind). Second set of four panels: sketch of the response of Janus colloids to the fields produced by other colloids with indications of which sign coefficients are required for the Keller-Segel (KS), Janus (Janus), and delay-induced (delay) instability. Right figure: universal phase diagram for quasi-2D repulsively interacting autophoretic colloids depending only on Péclet number (Pe) and area fraction (f). Lines show the onset of the delay-induced (blue) and Janus instability (red); the latter illustrates the case where colloids produce and consume and requires twice as large Pe numbers for pure producers; see [8].

induced rotation frequency in (an orthogonal) chemical-thermal unit gradient with rotational diffusion; (iii), (iv) $K_0 = k_0/D_r$; $K_d = k_d/D_r$, comparing production and decay rates of the phoretic field to D_r; and (v) $\mathcal{D} = D_c/(R_0^2 D_r)$, which measures the time scale that the phoretic field needs to diffuse over the radius of a colloid in units of the inverse rotational diffusion.

To understand the collective behavior of autophoretic colloids, we systematically derive a continuum theory [8] generating mean-field equations of motion for the particle density $\rho(\mathbf{x}, t)$ and the associated polarization density $\mathbf{w}(\mathbf{x}, t)$,

$$\dot{\rho} = -\mathrm{Pe}\nabla \cdot \mathbf{w},$$

$$\dot{\mathbf{w}} = -\mathbf{w} + \frac{B\rho}{2}\nabla c - \frac{\mathrm{Pe}}{2}\nabla\rho + \frac{\mathrm{Pe}^2}{16}\nabla^2\mathbf{w} - \frac{B^2|\nabla c|^2}{8}\mathbf{w}$$

$$+ \frac{\mathrm{Pe}B}{16}[3(\nabla\mathbf{w})^T \cdot \nabla c - (\nabla c \cdot \nabla)\mathbf{w} - 3(\nabla \cdot \mathbf{w})\nabla c],$$

$$\dot{c} = \mathcal{D}\nabla^2 c + K_0\rho + \nu\frac{K_0}{2}\nabla \cdot \mathbf{w} - K_d c. \qquad (4)$$

Here $\nu = 1$ for swimmers which move cap behind, and $\nu = -1$ for cap-ahead swimmers (Fig. 2). This model qualitatively resembles the phenomenological model considered in [3]; crucially, however, it provides a microscopic theory here linking all coefficients to microscopic quantities. It also features additional nonlinear terms, which do not affect the linear stability of the uniform phase and the corresponding nonequilibrium phase diagram, but *do* influence the emerging patterns.

Following [3], we expect different structure formation scenarios for colloids with attractive and repulsive phoretic interactions, which we now explore through linear stability analysis of the uniform solution $(\rho, \mathbf{w}, c) = (\rho_0, \mathbf{0}, K_0\rho/K_d)$ of (4). Specifically, attractive phoretic interactions induce the Keller-Segel (KS) instability described in the introduction if $(BK_0\rho_0)/(\mathrm{Pe}K_d) > 1$ [8]. Hence, strong coupling to the chemical field, fast production, and high particle

density all support this instability. While the KS instability is well established for microorganisms, our microscopic derivation shows that it also applies to autophoretic colloids.

Conversely, for $B < 0$ colloids effectively repel each other. If their phoretic production is anisotropic, as for Janus colloids, there is an instability inducing clusters of self-limiting size (see [3] for a discussion of the mechanism) which is effective if [8]

$$\frac{-B\nu K_0\rho_0(16\mathcal{D} + \mathrm{Pe}^2)}{(4\sqrt{2}\mathcal{D} + \mathrm{Pe}^2)^2} > 1. \qquad (5)$$

Remarkably, besides patterns emerging from the Janus instability, a delay in the response of the colloidal swimming direction can trigger a cyclic feedback loop resulting in wave formation [3], if [8]

$$\frac{-B\rho_0 K_0 \mathrm{Pe}}{2\mathcal{D}} > 1. \qquad (6)$$

To gauge the significance of (5) and (6) for real Janus colloids, we now reduce the parameter space further. For typical diffusiophoretic Janus swimmers $\mathcal{D} \sim 10^4 - 10^6 \gg 1$ ($\mathcal{D} \sim 10^6 - 10^8$ for thermophoretic swimmers), suggesting that the $\mathcal{D} \to \infty$ limit in (5) and (6) is physically relevant. However, naively taking this limit would rule out phoretic instabilities altogether. We now show why this approach is invalid and relate self-propulsion and phoretic cross-interactions allowing us to eliminate B, $\mathcal{D}$, and K_0 from our instability criteria. Consider a test particle exposed to the phoretic field c produced by other colloids. The gradient of c drives a surface slip velocity on our test particle $\mathbf{v}_s(\mathbf{r}_s) = \mu(\mathbf{r})\nabla_\parallel c(\mathbf{r})$ (in physical units) causing its rotation with a frequency $\mathbf{\Omega} = [3/(2R_0)]\langle \mathbf{v}_s(\mathbf{r}_s) \times \mathbf{n} \rangle$ [19] (self-rotations don't occur for homogeneous surface coatings). Here, $\nabla_\parallel c(\mathbf{r}) \equiv (\mathbb{1} - \mathbf{n}\mathbf{n}) \cdot \nabla c(\mathbf{r})$ is the projection of ∇c onto the plane tangent to the colloid with unit normal $\mathbf{n}(\mathbf{r})$, while brackets denote the surface average on the test colloid.

Performing this integration and assuming that $\boldsymbol{\nabla}c$ is constant on the scale of the test colloid (with orientation $\mathbf{p}$) yields $\boldsymbol{\Omega} = [3\nu/(8R_0)](\mu_C - \mu_N)\mathbf{p} \times \boldsymbol{\nabla}c$. Here, μ_C, μ_N are the phoretic surface mobilities on the catalytic and the neutral hemisphere of the test colloid, and $\mathbf{e}$ is the unit vector along its swimming direction. Comparing our expression for $\boldsymbol{\Omega}$ with (2) now yields $\beta = 3\nu(\mu_C - \mu_N)/(8R_0)$.

To eliminate from β the (usually unknown) mobility coefficients, we now calculate the phoretic field produced by each colloid. We solve the Laplace equation $D_c\nabla^2 c = 0$ with boundary conditions $-D_c\mathbf{n} \cdot \boldsymbol{\nabla}c = \alpha, 0$ on the catalytic and neutral caps, respectively, and $c(r \to \infty) = c_0$. This yields in far field $c(r) = c_0 + [(\alpha R_0^2)/(2D_c r)] + \mathcal{O}[R_0^3/(D_c r^2)]$. Besides acting on other colloids, this field also drives a (quasi-)slip velocity over the test colloid's own surface leading to self-propulsion with $\mathbf{v} = -\langle\mathbf{v}_s(\mathbf{r}_s)\rangle = -\langle\mu(\mathbf{r})\boldsymbol{\nabla}_{\|}c(\mathbf{r})\rangle \Rightarrow v = |\mathbf{v}| = \nu\alpha(\mu_C + \mu_N)/(8D_c)$ and $\nu = \text{sgn}[(\mu_N + \mu_c)\alpha]$ [19,20]. Combining the former with our previous expression for β gives $\beta = 3\mu_r D_c v/(R_0\alpha)$ with the reduced surface mobility $\mu_r = (\mu_C - \mu_N)/(\mu_C + \mu_N)$. Finally, we compare our expression for $c(r)$ with the steady-state solution of (3) (screened Poisson equation) for $N = 1$, $c = c_0 + [k_0/(4\pi D_c)][\exp(-\sqrt{k_d/D_c}\,r)/r]$. This gives $k_0 \gtrsim 2\pi R_0^2\alpha$ with equality for $k_d = 0$. Ultimately, using $|\mu_r| \approx 1$ for typical Janus colloids at $k_d = 0$ and $s := \text{sgn}(\mu_r)$, we find $\beta = 6\pi R_0\mu_r v D_c/k_0 \approx 6\pi R_0 s v D_c/k_0$ whereas $k_d > 0$ leads to larger β values. This key result translates to

$$B \approx \frac{6\pi s\text{Pe}\mathcal{D}}{K_0} \qquad (7)$$

in dimensionless units and has notable consequences. (i) For typical laser-heated thermophoretic swimmers, $\mu_C \approx 0$ [21], hence $B < 0$: such swimmers are (thermo)repulsive and therefore a candidate to observe in the laboratory the patterns predicted phenomenologically in [3] for repulsive phoresis. (ii) The parameter B linearly depends on $\mathcal{D}$. Thus, the naive approach of taking the $\mathcal{D} \to \infty$ limit while keeping B constant is inconsistent; phoretic patterns should remain observable even in the limit of fast diffusion. (iii) Crucially, Eq. (7) allows us to eliminate B from our instability criteria. Combining Eqs. (5)–(7), introducing the quasi-2D area fraction $f = \pi\rho_0$ ($f = \pi R_0^2\rho_0$ in physical units), and performing the limit $\mathcal{D} \to \infty$ [22] reduces the Janus and the delay-induced instability to

$$-3\nu s\text{Pe}f > 1 \quad \text{and} \quad -3s\text{Pe}^2 f > 1. \qquad (8)$$

Modulo sign coefficients s and ν, these instability criteria depend only on Pe and f [K_0 contributes only indirectly to (8) via Pe $\propto K_0/\mathcal{D}$ and K_d is insignificant if decay processes are not too fast [8]]. This massive parameter space collapse yields a universal phase diagram (Fig. 2) in which autophoretic colloids, with typical Pe ~ 20–200

[14–16], generically form patterns, even at low area fractions of $f \sim 0.01$. (The specific form of the emerging patterns, of course, still depends on all parameters.) Analogously, Eq. (7) reduces the KS instability for attractive autophoretic colloids to

$$6\mathcal{D}f > K_d. \qquad (9)$$

This criterion is fulfilled for $\mathcal{D} \gg 1$ and $K_d \ll 1$ (see the Supplemental Material [8] for $K_d > 1$). Hence, for both self-diffusiophoretic and self-thermophoretic Janus colloids, cross-phoretic interactions generically destabilize the uniform phase. This suggests that models based on purely local interactions such as the ABP model [18,23], are insufficient to capture the collective behavior of autophoretic systems; indeed, they predict the onset of structure formation at much higher area fractions than found experimentally [14–16].

Note that the PBP model describes only cross-phoretic *alignment* interactions and neglects cross-phoretic *drifts*. The latter are a separate source of long-range interactions [4,6], but lead only to order f^3 corrections of our instability criteria, Eq. (8). Physically, cross-phoretic drifts are insignificant at low densities as colloids drift slower in the $1/r^3$-decaying phoretic gradients produced by other colloids than in their self-produced gradients.

To test our key findings and to explore their robustness against short-ranged repulsions, we have solved Eqs. (1)–(3) numerically [8]. Attractive phoretic colloids undergo the KS instability and form small clusters at short times (Fig. 1(a), movie 1), which merge (b) and produce colocated phoretic clusters (c); these coarsen, eventually leaving a single cluster at steady state (not shown). This scenario applies even for area fractions $f \ll 0.01$ and is insensitive to parameter variations.

In contrast, repulsive phoretic interactions create a plethora of structures. In most cases, the delay-induced instability masks the Janus instability and creates continuously moving patterns. These involve colloidal waves pursued by self-produced phoretic waves; waves often morph into clusters and back to waves. At "early" times, which can last several hours in large systems, the delay-induced instability creates waves moving along randomly chosen directions [Fig. 1(g)] which coarsen to a characteristic scale (h, movies 2–4). When these waves collide frontally (movies 2 and 3), the pursuing phoretic waves act as cages for (repulsive) particles, compressing them into dense clusters (h, blue rectangle). The high particle density within the clusters enhances the phoretic production, leading, a short while after, to colocated phoretic clusters (i). The high phoretic field then expels the colloids, inducing cluster explosions, initiating new colloidal ring waves leaving low density regions at the locations of the former clusters (j). These waves continue to collide generating a rich pattern of exploding and traveling clusters

(the latter emerge from less frontal collisions, movie 3) and of waves sometimes spontaneously changing their direction of motion. At late times, this type of motion can settle down into a regular pattern of moving bands which are closely pursued by self-produced chemical or heat bands; this late-time pattern can be best observed in elongated simulation boxes (k,l, movie 4).

Finally, we consider a variant of the PBP model in which colloids produce a phoretic field on one hemisphere and consume it with the same rate on the other. This yields $c \propto 1/r^2$ in far field, but leaves (7) unchanged modulo order-one prefactors. Such zero-net-production (ZNP) colloids might mimic self-electrophoretic swimmers in which a current flows between hemispheres to give a $1/r^2$ far field (see [24]). They might also model Janus particles whose self-diffusiophoretic motion hinges on a nonlinear threshold effect as might arise in the laser-induced local demixing of a binary fluid near the cap [16,25]. Interestingly, for ZNP swimmers the Janus instability is no longer preempted by the delay-induced instability (Fig. 2) which requires net phoretic production. Our simulations (Figs. 1(d–f), movie 5) yield dynamic clusters which are surrounded by self-produced phoretic shells (e) and do not coarsen beyond a certain scale, but continuously emerge and disrupt without ever settling into a steady state. This phenomenology resembles the living clusters observed in [14,15].

In conclusion, the fact that autophoretic colloids swim obliges them to form patterns. Both attractive and repulsive cross-phoretic interactions *generically* induce structure formation in self-diffusiophoretic and self-thermophoretic Janus colloids, even at very low densities. This relies on a collapse of parameter space, applying when the lifetime of the phoretic field is not too small compared to the persistence time of a swimmer.

While we expect that hydrodynamic interactions [26,27] will not change our finding that phoretic interactions generically destabilize the uniform phase, they will influence the emerging patterns and, in particular, their length scales. Similarly, our phase diagram should be invariant to fuel depletion which might, however, induce notable late-time effects once dense clusters and waves have emerged. Hence, further studies will be needed to clarify the relation between our phoretic patterns and living clusters.

*corresponding author.
Benno.Liebchen@ed.ac.uk, bliebche@gmail.com

[1] E. F. Keller and L. A. Segel, J. Theor. Biol. **26**, 399 (1970).
[2] E. F. Keller and L. A. Segel, J. Theor. Biol. **30**, 225 (1971).
[3] B. Liebchen, D. Marenduzzo, I. Pagonabarraga, and M. E. Cates, Phys. Rev. Lett. **115**, 258301 (2015).
[4] S. Saha, R. Golestanian, and S. Ramaswamy, Phys. Rev. E **89**, 062316 (2014).
[5] M. Meyer, L. Schimansky-Geier, and P. Romanczuk, Phys. Rev. E **89**, 022711 (2014).
[6] O. Pohl and H. Stark, Phys. Rev. Lett. **112**, 238303 (2014).
[7] B. Liebchen, M. E. Cates, and D. Marenduzzo, Soft Matter **12**, 7259 (2016).
[8] See Supplemental Material at http://link.aps.org/supplemental/10.1103/PhysRevLett.118.268001, which includes Refs. [9–11], for details on the kinetic theory, the phoretic production process and linear stability analyses.
[9] J. L. Willems, *Stability Theory of Dynamical Systems* (Wiley Interscience Division, New York, 1970).
[10] D. Dean, J. Phys. A **29**, L613 (1996).
[11] E. Bertin, M. Droz, and G. Grégoire, J. Phys. A **42**, 445001 (2009).
[12] H.-R. Jiang, N. Yoshinaga, and M. Sano, Phys. Rev. Lett. **105**, 268302 (2010).
[13] C. Jin, C. Krüger, and C. C. Maass, Proc. Natl. Acad. Sci. **114**, 5089 (2017).
[14] I. Theurkauff, C. Cottin-Bizonne, J. Palacci, C. Ybert, and L. Bocquet, Phys. Rev. Lett. **108**, 268303 (2012).
[15] J. Palacci, S. Sacanna, A. P. Steinberg, D. J. Pine, and P. M. Chaikin, Science **339**, 936 (2013).
[16] I. Buttinoni, J. Bialké, F. Kümmel, H. Löwen, C. Bechinger, and T. Speck, Phys. Rev. Lett. **110**, 238301 (2013).
[17] J. Bialké, T. Speck, and H. Löwen, J. Non-Cryst. Solids **407**, 367 (2015).
[18] M. E. Cates and J. Tailleur, Annu. Rev. Condens. Matter Phys. **6**, 219 (2015).
[19] J. L. Anderson, Annu. Rev. Fluid Mech. **21**, 61 (1989).
[20] R. Golestanian, T. B. Liverpool, and A. Ajdari, New J. Phys. **9**, 126 (2007).
[21] T. Bickel, A. Majee, and A. Würger, Phys. Rev. E **88**, 012301 (2013).
[22] Taking this limit is for convenience only; large Péclet numbers $Pe^2 > \mathcal{D}$ further support instability.
[23] P. Romanczuk, M. Bär, W. Ebeling, B. Lindner, and L. Schimansky-Geier, Eur. Phys. J **202**, 1 (2012).
[24] A. T. Brown, W. Poon, C. Holm, and J. de Graaf, Soft Matter **13**, 1200 (2017).
[25] I. Buttinoni, G. Volpe, F. Kümmel, G. Volpe, and C. Bechinger, J. Phys. Condens. Matter **24**, 284129 (2012).
[26] A. Scagliarini and I. Pagonabarraga, arXiv:1605.03773.
[27] M. Wagner and M. Ripoll, arXiv:1701.07071v1.